



Influence of Switchgrass *TDIF*-like Genes on *Arabidopsis* Vascular Development

Dongdong Tian^{1,2}, Jingwen Tang¹, Liwen Luo¹, Zhe Zhang¹, Keping Du^{1,3}, Robert M. Larkin¹, Xueping Shi^{1,3*} and Bo Zheng^{1,3*}

¹ Key Laboratory of Horticultural Plant Biology of Ministry of Education, College of Horticulture and Forestry Sciences, Huazhong Agricultural University, Wuhan, China, ² Tobacco Research Institute, Chinese Academy of Agricultural Science, Qingdao, China, ³ Hubei Engineering Technology Research Center for Forestry Information, Huazhong Agricultural University, Wuhan, China

OPEN ACCESS

Edited by:

Qingyu Wu,

Chinese Academy of Agricultural Sciences (CAAS), China

Reviewed by:

Alison W. Roberts,

University of Rhode Island,

United States

Guodong Wang,

Shaanxi Normal University, China

*Correspondence:

Xueping Shi

xpshi@mail.hzau.edu.cn

Bo Zheng

bo.zheng@mail.hzau.edu.cn

Specialty section:

This article was submitted to

Plant Physiology,

a section of the journal

Frontiers in Plant Science

Received: 06 July 2021

Accepted: 17 August 2021

Published: 23 September 2021

Citation:

Tian D, Tang J, Luo L, Zhang Z, Du K, Larkin RM, Shi X and Zheng B (2021)

Influence of Switchgrass *TDIF*-like Genes on *Arabidopsis* Vascular Development.

Front. Plant Sci. 12:737219.

doi: 10.3389/fpls.2021.737219

As a member of the *CLAVATA3* (*CLV3*)/*EMBRYO SURROUNDING REGION* (*CLE*) family, the dodecapeptide tracheary element differentiation inhibitory factor (*TDIF*) has a major impact on vascular development in plants. However, the influence of polymorphisms in the *TDIF* peptide motif on activity remains poorly understood. The model plant, *Arabidopsis* provides a fast and effective tool for assaying the activity of *TDIF* homologs. Five *TDIF* homologs from a group of 93 *CLE* genes in switchgrass (*Panicum virgatum*), a perennial biomass crop, named *PvTDIF*-like (*PvTDIFL*) genes were studied. The expression levels of *PvTDIFL1*, *PvTDIFL3^{MR3}*, and *PvTDIFL3^{MR2}* were relatively high and all of them were expressed at the highest levels in the rachis of switchgrass. The precursor proteins for *PvTDIFL1*, *PvTDIFL3^{MR3}*, and *PvTDIFL3^{MR2}* contained one, three, and two *TDIFL* motifs, respectively. Treatments with exogenous *PvTDIFL* peptides increased the number of stele cells in the hypocotyls of *Arabidopsis* seedlings, with the exception of *PvTDIFL_4p*. Heterologous expression of *PvTDIFL1* in *Arabidopsis* strongly inhibited plant growth, increased cell division in the vascular tissue of the hypocotyl, and disrupted the cellular organization of the hypocotyl. Although heterologous expression of *PvTDIFL3^{MR3}* and *PvTDIFL3^{MR2}* also affected plant growth and vascular development, *PvTDIFL* activity was not enhanced by the multiple *TDIFL* motifs encoded by *PvTDIFL3^{MR3}* and *PvTDIFL3^{MR2}*. These data indicate that in general, *PvTDIFLs* are functionally similar to *Arabidopsis* *TDIF* but that the processing and activities of the *PvTDIFL* peptides are more complex.

Keywords: switchgrass, *CLE*, *TDIF*, vascular development, biomass

INTRODUCTION

In plants, the *CLAVATA3* (*CLV3*)/*EMBRYO SURROUNDING REGION* (*CLE*) gene family plays a vital role in cell division and cell differentiation by mediating intercellular communication (Fletcher et al., 1999; Fiers et al., 2005, 2007). *CLE* peptides are derived from a pre-propeptide containing an N-terminal signal peptide and a conserved C-terminal motif of 12–13 amino acids. A few *CLE* genes encode multiple *CLE* motifs in rice, wheat (*Triticum aestivum*), *Picea*, and *Amborella*, etc. (Goad et al., 2017). *CLE* genes are ubiquitous in the plant kingdom, and have been comprehensively studied in eudicots (*Arabidopsis thaliana*, *Glycine max*, *Lycopersicon esculentum*,

Gossypium hirsutum, *Populus trichocarpa*, and *Vitis vinifera*), monocots (*Oryza sativa*, *T. aestivum*, and *Zea mays*), and gymnosperms (*Picea abies* and *P. glauca*) (Cock and McCormick, 2001; Sawa et al., 2008; Strabala et al., 2014; Han et al., 2016; Goad et al., 2017; Wang et al., 2019). In *A. thaliana*, at least 32 *CLE* genes have been identified (Ito et al., 2006; Kondo et al., 2006; Ohyama et al., 2009; Ogawa-Ohnishi et al., 2013). Based on their biological functions, the *Arabidopsis* *CLE* peptides were grouped into two major classes. The A-type *CLE* peptides which maintain the apical meristems in shoots and roots and include *CLV3*, *CLE1-27*, and *CLE40*. The B-type/H-type *CLE* peptides, on the other hand, suppress xylem differentiation and promote vascular procambial cell division and include *CLE41*, *CLE42*, and *CLE44* (Schoof et al., 2000; Ito et al., 2006; Whitford et al., 2008; Stahl et al., 2009; Hirakawa et al., 2010a,b).

One member of the *CLE* family, a dodecapeptide (H-E-V-P-S-G-P-N-P-I-S-N) named tracheary element differentiation inhibitory factor (TDIF) was first identified in a *Zinnia elegans* mesophyll cell xylogenesis system. H¹ is unique among *CLE* peptides with TDIF activity, and V³, N⁸, and N¹² are essential for TDIF activity (Ito et al., 2006). In *Arabidopsis*, TDIF is encoded by two genes, *CLE41* and *CLE44*. *CLE42* and *CLE46* are classified as *TDIF-like* (*TDIFL*) genes, because their *CLE* motifs (H-G-V-P-S-G-P-N-P-I-S-N and H-K-H-P-S-G-P-N-P-T-G-N, respectively) are highly homologous to the TDIF motif. The *TDIF* genes are mainly involved in the regulation of vascular development. The TDIF signaling pathway in the vascular meristem has been well-studied (Ito et al., 2006; Ohyama et al., 2008). The TDIF RECEPTOR/PHLOEM INTERCALATED WITH XYLEM (TDR/PXY), a member of the leucine-rich repeat receptor-like kinase (LRR-RLK) family, is the TDIF receptor in procambial cells (Fisher and Turner, 2007; Hirakawa et al., 2008). The TDIF peptide that is produced in the phloem controls vascular procambial or cambial cell proliferation and xylem differentiation by activating TDR/PXY in the procambium or cambium. Two transcription factors, WUSCHEL HOMEODOMAIN RELATED 4 (*WOX4*) and *WOX14*, regulate the proliferation of plant vascular tissue by acting downstream of the TDIF-TDR/PXY signaling pathway (Hirakawa et al., 2010a,b; Etchells et al., 2013; Kucukoglu et al., 2017; Li et al., 2018). In addition, an NAC domain transcription factor, *XVP*, fine-tunes the TDIF signaling that contributes to vascular development by serving as a negative regulator (Kucukoglu, 2020; Yang et al., 2020). Current reports on TDIF/TDIFL have focused on genes encoding a single motif. Little is known about the function of TDIF/TDIFL genes encoding multiple motifs.

Switchgrass (*P. virgatum*) is a highly productive herbaceous perennial that thrives in diverse environments and is, therefore, a model perennial biomass crop (PBC) (Sanderson et al., 1996; McLaughlin and Adams Kszos, 2005). It has been a feedstock for the biofuels and specialty chemicals (Parrish and Fike, 2005; Sanderson et al., 2006; Keshwani and Cheng, 2009). Among the four PBCs (poplar, switchgrass, *Miscanthus*, and *Salix*), molecular regulation of lignocellulosic formation has been comprehensively studied in poplar trees (Clifton-Brown et al., 2019). Increasing vascular cambial activity results in incremental xylem and phloem, therefore increasing the biomass of wood. The division

of vascular cambial cells was stimulated by manipulating *CLE41*-*PXY* signaling in hybrid poplar (Etchells and Turner, 2010; Etchells et al., 2015). The *WOX4* controls the rate of cambial cell division and hence, the growth of stem girth in a TDIF-dependent manner (Kucukoglu et al., 2017). In a recent report, the *CLE* gene family in switchgrass, including three *PvTDIFL* genes, was defined. The statistical analysis demonstrated that no common TDIF/TDIFL motif is shared between monocots and dicots and that the contribution of TDIF/TDIFL to the development of vascular tissue has probably been diverged in monocots and dicots (Zhang et al., 2020). However, the knowledge of TDIF/TDIFL peptide functions in switchgrass remains limited.

Studying the mechanisms that drive rapid growth in switchgrass and other PBCs may help to introduce biomass-related genes, pathways or regulatory modules into dicotyledonous plants. *Arabidopsis* is widely used in the study of secondary cell wall formation and vascular development because although *Arabidopsis* is an annual herbaceous plant, it has most of the cell types associated with secondary growth (Zhang et al., 2011; Ursache et al., 2013; Ragni and Hardtke, 2014). The TDIF-TDR/PXY signaling pathway has been well-studied in *Arabidopsis* (Etchells and Turner, 2010; Hirakawa et al., 2010a,b; Etchells et al., 2013, 2016; Wang et al., 2013; Kondo and Fukuda, 2015; Zhang et al., 2016; Kucukoglu, 2020). Thus, *Arabidopsis* is suitable for activity screening and functional analysis of *TDIF/TDIFL* genes from various plants. This study aimed to use bioinformatics tools to identify the *CLE* gene family, including *TDIF/TDIFL* genes, at the whole genome level in *P. virgatum*. Treatment of *Arabidopsis* with exogenous TDIF/TDIFL peptides and heterologous expression of *TDIF/TDIFL* genes in *Arabidopsis* allowed the researchers of this study to test whether particular PvTDIFL peptides influenced plant growth and vascular development. Rapid characterization of PvTDIFL peptides in *Arabidopsis* can provide a preliminary understanding of the biological activities of PvTDIFL peptides and indicate potential biotechnological applications related to wood formation and biomass improvement. This is not practical to achieve with switchgrass because the genetic transformation of switchgrass is still time-consuming and laborious (Xi et al., 2009; Chen and Song, 2019; Ondzighi-Assoume et al., 2019).

MATERIALS AND METHODS

Identification of *CLE* Genes in *P. virgatum*

The amino acid sequences of *Arabidopsis* *CLE* proteins were downloaded from The *Arabidopsis* Information Resource (TAIR) (<https://www.Arabidopsis.org/>). The 12-amino acid *CLE* motifs were used as queries in TBLASTN search of the *P. virgatum* v1.1 genome with a threshold e-value of 500 in the Phytozome v12.1 database (<https://phytozome.jgi.doe.gov/pz/portal.html>) (Goodstein et al., 2012). Repeated hits were removed and only one hit at each chromosomal location was kept. Genes at each chromosomal location were identified as potential *CLE* genes. If there was no annotated gene at the target location, a 5-kb genome fragment with the target location in the center was then retrieved and subjected to an analysis with the online software, FGENSESH,

for gene predictions on the softberry website (<http://linux1.softberry.com/>) (Solovyev et al., 2006). Amino acid sequences encoded by each of the potential *CLE* genes were checked for the C-terminal conserved *CLE* motifs. All of the newly identified motifs were used as queries in TBLASTN searches, as described in the preceding steps. The analysis was iterated until no more *CLE* candidate could be identified. All of the *CLE* candidates were compared with the previously reported *CLE* genes in *P. virgatum* (Zhang et al., 2020). The final *TDIF/TDIFL* gene sequences were obtained using cloning based on the nucleotide sequences from Phytozome (**Supplementary Figure 1**).

Bioinformatics Analysis

To classify *PvCLE* genes, all 12-aa *CLE* motifs encoded by *AtCLE* and *PvCLE* genes were extracted, including the *PvCLE* genes encoding multiple *CLE* motifs. Phylogenetic trees containing the 12-aa *CLE* motif sequences were constructed as previously described (Zhang et al., 2020). Based on the clustering of *CLE* motifs, *PvCLE* genes in the same group as *AtTDIF/TDIFL* genes were predicted as *PvTDIFL* genes. To further analyze the evolutionary relationship between *PvTDIFL* and *AtTDIF/TDIFL* genes, phylogenetic trees containing the full-length amino acid sequences for *TDIF/TDIFL* from both *P. virgatum* and *Arabidopsis* were constructed using the MEGA 5.05 software (Hall, 2013) with the following parameters: alignment, Muscle, phylogeny construct or test, Maximum Likelihood Tree, and number of bootstrap replication = 1000. Signal peptides that target the *TDIF/TDIFL* proteins to the secretory pathway were predicted with the SMART Server using a normal model (http://smart.embl-heidelberg.de/smart/set_mode.cgi?NORMAL=1) (Letunic and Bork, 2018). Gene structure analysis was performed using the Gene Structure Display Server 2.0 (<http://gsds.cbi.pku.edu.cn/>) (Hu et al., 2015). The Format of Gene Features was set as fast-all (FASTA) Sequence. Other features containing signal peptides and motifs were uploaded in Browser Extensible Data (BED) format. Phylogenetic Tree was uploaded in Newick format based on full-length amino acid sequences (Hu et al., 2015). Multiple alignments were performed using the DNAMAN v6.0 software (Lynnon Biosoft, Quebec, Canada). Weblogo-Create Sequence Logos (<http://weblogo.berkeley.edu/logo.cgi>) was used for comparative analysis of motif conservation and for conservation analysis of each amino acid site of *TDIF/TDIFL* motifs in *Arabidopsis* and switchgrass (Crooks et al., 2004). Isoelectric point (*pI*) and molecular weight (*MW*) were calculated using the ExpAsy-ProtParam tool (<http://web.expasy.org/protparam/>) (Bjellqvist et al., 1993).

Plant Materials and Growth Conditions

Arabidopsis thaliana ecotype Columbia-0 (Col-0) and *P. virgatum* were used in this study. *Arabidopsis* seeds were surface sterilized in 75% (v/v) ethanol for 1 min and 5% (v/v) sodium hypochlorite for 15 min, with occasional gentle shaking. The seeds were then washed five times with sterilized distilled H₂O (dH₂O). After stratification at 4°C for 2 days, the seeds were placed in liquid Murashige and Skoog (MS) medium (pH 5.8) containing 1.5% sucrose (w/v) or on solid MS medium (pH

5.8) containing 1.5% sucrose (w/v) and 0.7% plant agar (w/v). The conical flasks containing liquid medium and the plates containing solid medium were placed in a tissue culture room maintained at 23°C and grown in a photoperiod containing 16 h of light at a fluence rate of 100 μmol photons m⁻² s⁻¹ followed by 8 h of dark. The conical flasks were placed on an orbital shaker at a rotational speed of 80 rpm. The plates were positioned vertically. *Arabidopsis* were grown in soil under the same temperature and light conditions, except that light intensity was set as 150 μmol photons m⁻² s⁻¹. The *P. virgatum* plants used in this study were grown at Huazhong Agricultural University, Wuhan, China.

Exogenous Peptide Treatment

The *TDIF/TDIFL* peptides derived from *Arabidopsis* *TDIF* and *PvTDIFL* motifs (**Supplementary Table 1**) were chemically synthesized by GenScript Biotech Corporation (Nanjing, China). Twenty milligrams of each peptide was provided at a purity ≥ 90% (w/w). Peptides were dissolved in double distilled water (ddH₂O) at a stock concentration of 1 mg/ml and stored at -80°C for future use. Synthetic *TDIF* and *PvTDIFL* peptides were added to liquid medium at a final concentration of 10 μM as previously described (Whitford et al., 2008). *Arabidopsis* seeds were treated with 10 ml of medium in conical flasks on an orbital shaker at a rotational speed of 80 rpm for 10 days. Each treatment required six flasks, with six seeds per flask.

RNA Extraction and qRT-PCR Analysis of *PvTDIFL* Genes

Five different tissues of *P. virgatum*, namely, seed (mature seeds), rachis (bearing mature seeds), leaf (fully expanded leaf), stem (middle internode of seedling), and root were sampled in triplicates and immediately frozen in liquid nitrogen. Total RNA was extracted using the 2 × CTAB method (Li et al., 2008). The pellet was dissolved in 30 μl of RNase free ddH₂O. The concentration and quality of RNA were measured with a NanoDrop[®] 2000 spectrophotometer (Thermo Scientific, Wilmington, Delaware, USA). The RNA samples with A₂₆₀/A₂₈₀ ratios that ranged from 1.8 to 2.1 and A₂₆₀/A₂₃₀ ratios ≥ 2 were stored at -80°C for future use.

To quantify the relative expression levels of *PvTDIFL* genes in different samples, 1 μg of total RNA was used as a template to synthesize cDNA using the PrimeScript[™] RT reagent Kit with gDNA Eraser (Perfect Real Time) (TaKaRa, Dalian, China). The qRT-PCR reactions were then prepared using 2 × HSYBR qPCR Mix without ROX (ZOMANBIO, Beijing, China). A standard 2-step amplification protocol was run in a LightCycler[®] 96 Real-Time PCR System (Roche, USA). The comparative C_T method (ΔΔC_T method) was used for relative quantification of real-time PCR (Pfaffl, 2001). *PvUBQ6* (Pavir.5NG345900) was used as the reference gene (Gimeno et al., 2014). All gene specific primers (**Supplementary Table 2**) were designed using the Primer Premier 5.0 software (www.PremierBiosoft.com). All real-time PCR reactions were run in three biological replicates and two technical replicates.

Plasmid Construction and Generation of Transgenic Plants

The coding sequences (CDS) from *PvTDIFL3*^{MR3} and *PvTDIFL3*^{MR2} were amplified using PCR with gene specific primers (Supplementary Table 2). The CDS of *PvTDIFL1* was artificially synthesized (Sunny Technology, Shanghai, China). The products were cloned into a Gateway™ entry vector *pDONR201* using the BP recombination reaction (Invitrogen). The clones were analyzed using DNA sequencing. The correct fragments were subsequently recombined into the destination vector, *pK2GW7* (Karimi et al., 2002). Transformation of *A. thaliana* was performed using the *Agrobacterium tumefaciens*-mediated floral dip method (Clough and Bent, 1998).

Morphological and Histological Analysis of Arabidopsis Seedlings

Arabidopsis seedlings were photographed with a Canon EOS 7D digital camera to obtain high-resolution images. Root length was measured by using the ImageJ software (<http://imagej.nih.gov/ij>). The images presented in the figures were representative images from images of 24 individual seedlings for each line for the plate-grown plants and 10 individual seedlings for each line for the soil-grown plants, respectively.

Histological analysis of the vasculature was performed by using semi-thin sections. The upper part of the hypocotyl, 2–3 mm in length, was cut with a scalpel. A small amount of tissue from the stem and petiole of the rosette was kept to mark the upper end of the hypocotyl segment. The hypocotyl segments were fixed in formalin-acetic acid-alcohol (FAA) fixative (50% ethanol, 10% glacial acetic acid, 5% formaldehyde, v/v/v) at 4°C for 24 h. Dehydration was carried out by immersing the specimen in an ascending series of ethanol. Lastly, the specimens were infiltrated and embedded with Technovit® 7100 resin (www.kulzer-technik.com). The hypocotyl specimens were transversely sectioned at a thickness of 2.5 μm using a RM2265 Microtome (Leica BIOSYSTEMS, Nussloch, Germany) beginning from the upper end. The rosette tissues were first trimmed and monitored by sectioning and microscopy. The 10th to 20th sections of the hypocotyls were stained with 0.05% (w/v) aqueous toluidine blue and visualized with a BX53 light microscope (OLYMPUS, Tokyo, Japan). The cells in the stele were marked by using the ImageJ software and the number of cells was counted manually.

Statistical analysis was performed with six biological replicates and a *t*-test was used with double sample variance assumption. The letters a, b, and c and asterisks indicate statistically significant differences relative to the control.

Accession Numbers

Sequence data from this article are from the *P. virgatum* v1.1 genome in the Phytozome v12.1 database and TAIR10 associated with the following accession numbers: *AtEF1-α* (AT5G60390), *PvUBQ6* (Pavir.5NG345900), *AtCLE41* (AT3G24770), *AtCLE42* (AT2G34925), *AtCLE44* (AT4G13195), *AtCLE46* (AT5G59305), *PvTDIFL1* (Pavir.Ab03264), *PvTDIFL2* (Pavir.Aa00134), and

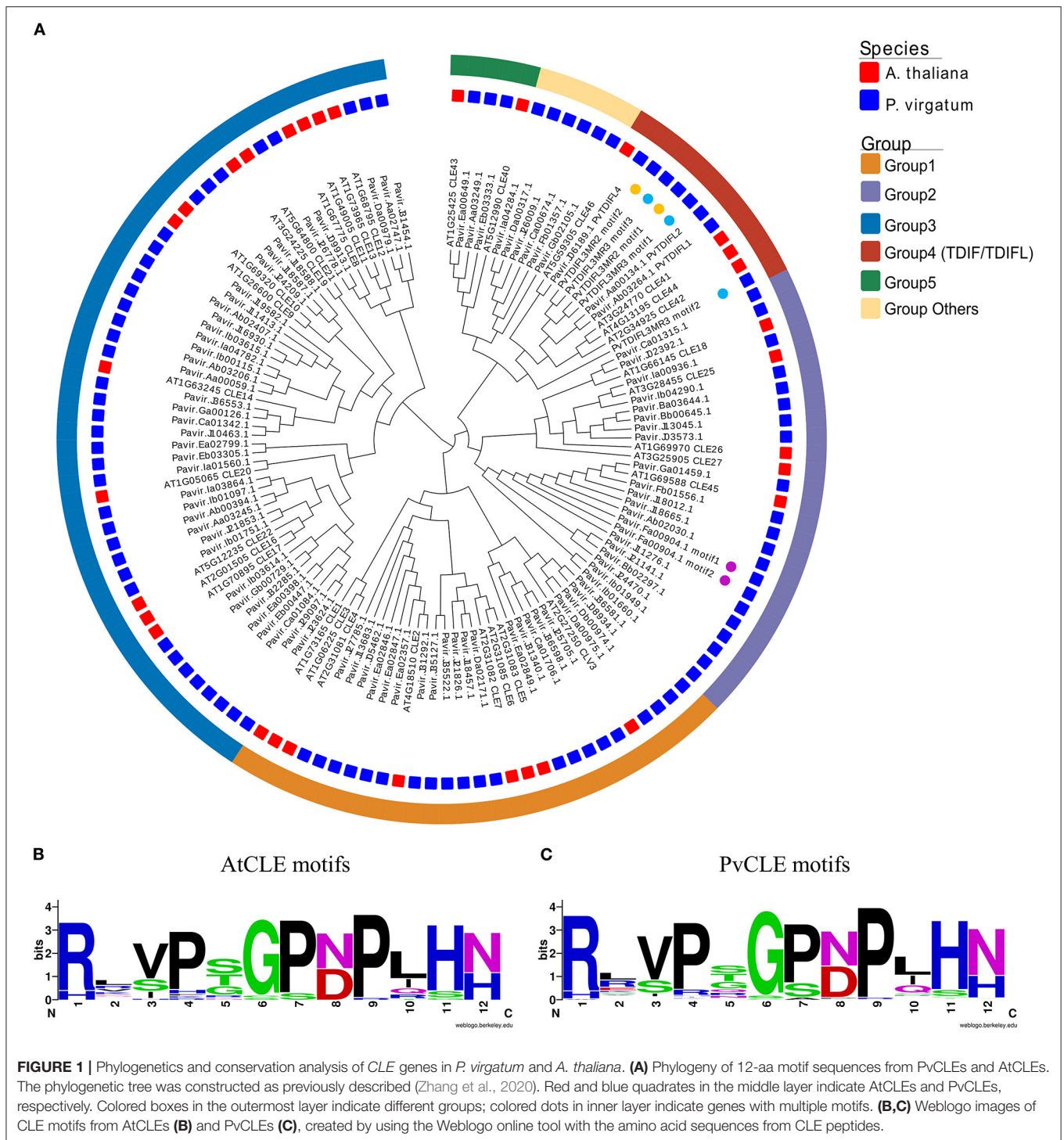
PvTDIFL4 (Pavir.J06189). The sequence data for *PvTDIFL3*^{MR3} and *PvTDIFL3*^{MR2} has been submitted to GenBank and are associated with accession numbers MZ463198 and MZ463199, respectively.

RESULTS

Identification of CLE Genes in *P. virgatum*

To identify *CLE* genes in *P. virgatum* (*PvCLE*), sequences similar to the *Arabidopsis* *CLE* motifs were identified in the *P. virgatum* v1.1 genome (<https://phytozome.jgi.doe.gov/pz/portal.html>). The *PvCLE* genes were predicted and clustered using the recently reported method (Zhang et al., 2020). In total, 93 *PvCLE* genes were identified, including 91 annotated *PvCLEs* in the *P. virgatum* v1.1 genome and two novel *PvCLEs* identified in this study (Figure 1, Supplementary Table 3). Since there were three *PvCLEs* that encoded multiple *CLE* motifs, all *PvCLEs* encoded a total of 97 *CLE* motifs. The total number of *PvCLEs* was nearly three times of the number of *AtCLEs*. Based on the clustering, *PvCLEs* were divided into six groups (Figure 1A, Supplementary Figure 2). The Weblogo of *CLE* motifs showed that Group 1, including eight *AtCLEs* (*AtCLE1-7*, and *AtCLV3*) and 21 *PvCLEs*, had two conserved amino acids, namely, Asp (D) at the 8th residue and His (H) at 12th residue. These two residues were replaced with Asn (N) in Group 3, which contained 13 *AtCLEs* (*AtCLE8-14*, *AtCLE16-17*, and *AtCLE19-22*) and 38 *PvCLEs*. Residue number 12 was Asn (N) in Group 2, which contained five *AtCLEs* (*AtCLE18*, *AtCLE25-27*, and *AtCLE45*) and 20 *PvCLEs* (Supplementary Figure 2). The Pavir.Fa00904.1 from Group 2 encoded two repeats of RRVRGSDPIHN, therefore the Group 2 *PvCLEs* encoded a total of 21 *CLE* motifs. Group 4 was comprised of nine *TDIF/TDIFL* genes, with four members from *Arabidopsis* (*AtCLE41*, 42, 44, and 46) and five genes from *P. virgatum*. In Group 4, there were two *PvCLEs* encoding multiple *TDIFL* motifs (see the next paragraph for details), and the total number of *TDIFL* motifs encoded in *P. virgatum* was as many as eight. Group 5 had two *Arabidopsis* members (*AtCLE40* and *AtCLE43*) and three *PvCLEs*. In general, the motif conservation in Group 5 was lower relative to groups 1 through 4. Six *PvCLE* genes were found upon encoding *CLE* motifs that are very different from the *AtCLE* motifs and thus, fell into “Group others” (Figure 1A, Supplementary Table 3). The *CLE* motifs are rather conserved between the *AtCLEs* and *PvCLEs* (Figures 1B,C).

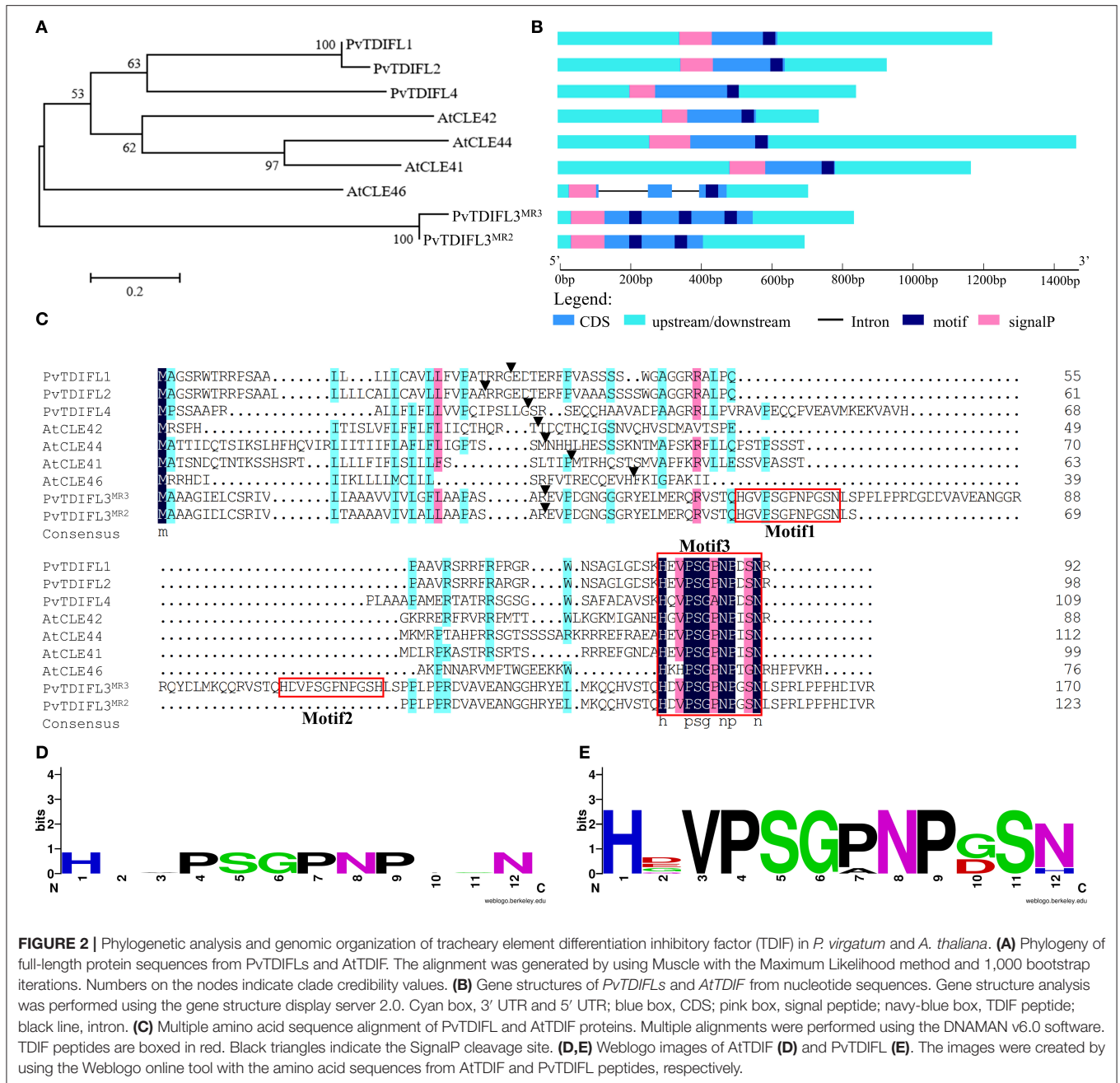
In total, five *TDIF* homologous genes were identified in the *P. virgatum* genome (Figure 2, Supplementary Figure 1, Table 1). The three *TDIF* homologs that were annotated are Pavir.Ab03264, Pavir.Aa00134, and Pavir.J06189, namely *PvTDIF-like1* (*PvTDIFL1*), *PvTDIFL2*, and *PvTDIFL4* in this study, respectively. A novel *TDIFL* gene, *PvTDIFL3*, was identified from TBLASTN searches of the *P. virgatum* v1.1 genome with a threshold *e*-value of 500. The predicted *PvTDIFL3* protein product contained three potential *TDIFL* motifs and hence named *PvTDIFL3*^{MR3}. The MR3 is referring to that it has three motif repeats (Figure 2, Table 1). When gene-specific primers were used to amplify the CDS of *PvTDIFLs*, a shorter fragment derived from *PvTDIFL3*^{MR3} was also cloned that was



named *PvTDIFL3^{MR2}* (Figures 2A–C). The amino acid sequence of *PvTDIFL3^{MR2}* is identical to that of *PvTDIFL3^{MR3}*, except that 47 amino acid residues are missing from the middle. The missing 47 amino acid residues constitute the second TDIFL motif and its flanking sequences of *PvTDIFL3^{MR3}* (Figure 2C). The *PvTDIFL3^{MR2}* matched to the same chromosomal location as *PvTDIFL3^{MR3}* in TBLASTN search of the *P. virgatum* v1.1 genome. In a phylogenetic analysis, amino acid sequences from

the five *PvTDIFL* genes clustered in the same clade as the amino acid sequences from *Arabidopsis TDIF/TDIFL* genes (Figures 1, 2A). The nucleotide sequences were subjected to the online gene prediction program FGENESH on the Softberry website (<http://linux1.softberry.com/>), to evaluate the genomic sequence and gene structure of these five genes.

All the TDIF/TDIFL proteins from *Arabidopsis* and switchgrass contained a signal peptide for the secretory pathway



at the N-terminus (**Figures 2B,C**). Similar to the *Arabidopsis* TDIF proteins, PvTDIFL1, 2, and 4 had a single TDIFL motif at the C-terminus. However, PvTDIFL3^{MR3} and PvTDIFL3^{MR2} had three and two TDIFL motifs, respectively (**Figures 2B,C**). The PvTDIFL proteins ranged from 92 to 175 amino acid residues in length. Their theoretical molecular weights (MW) and isoelectric points (pI) ranged from 10.01 to 18.50 kDa and from 5.81 to 11.94, respectively (**Table 1**).

A multiple sequence alignment analysis revealed that PvTDIFL1 and 2 proteins shared the same motif, HEVPSGPNPDSN, which is different from the *Arabidopsis*

TDIF motif at the 10th residue in that an Ile (I) residue is changed to an Asp (D) residue. Motif 1 and motif 3 of PvTDIFL3^{MR3}/PvTDIFL3^{MR2} were different at the 2nd and 10th residues relative to the TDIF motif. The 12th residue of Motif 2 from PvTDIFL3^{MR3} had an Asn (N) to His (H) substitution. The 2nd, 7th, and 10th residues of the motif from PvTDIFL4 were different from the TDIF motif (**Figure 2C**). The conserved TDIF/TDIFL dodecapeptides in *Arabidopsis* and switchgrass were compared by using a WebLogo analysis. Similar to the *Arabidopsis* TDIF, the 4th and 7th residues of the TDIFL motifs in PvTDIFL proteins were conserved Pro (P) residues.

TABLE 1 | Information of PvTDIFL peptides used in this study.

Protein symbol	Gene ID	Protein length (AA)	SignalP cleavage site	Position of motif (AA)	PvTDIFL motif
PvTDIFL1	Pavir.Ab03264	92	31	80-91	HEVPSGPNPDSN
PvTDIFL2	Pavir.Aa00134	98	31	86-97	HEVPSGPNPDSN
PvTDIFL3 ^{MR3}	NA	171	32	56-67 103-114 146-157	HGVPSGPNPGSN HDVPSGPNPGSH HDVPSGPNPGSN
PvTDIFL3 ^{MR2}	NA	124	32	56-67 99-110	HGVPSGPNPGSN HDVPSGPNPGSN
PvTDIFL4	Pavir.J06189	109	26	98-109	HQVPSGANPDSN

NA, indicates no annotation.

However, their 2nd, 10th and 12th residues were less conserved (Figures 2D,E).

Tissue-Specific Expression Analysis of PvTDIFL Genes in *P. virgatum*

In *Arabidopsis*, *CLE41* is expressed in the phloem and the neighboring pericycle cells in the root and hypocotyl. *CLE44* is expressed in the phloem, pericycle and endodermal cells (Hirakawa et al., 2008). To analyze the expression pattern of PvTDIFL genes in the different tissues of switchgrass, *in silico* expression analysis and qRT-PCR were both performed.

The *in silico* expression data for PvTDIFL1, 2, and 4 were downloaded from Phytozome. PvTDIFL1 and 2 were both expressed at the highest levels in the inflorescence panicle, rachis and shoot. The PvTDIFL3^{MR3} and PvTDIFL3^{MR2} were not annotated in Phytozome and thus, no *in silico* expression data was available. The expression of PvTDIFL4 was barely detectable in the tissues studied (Figure 3A).

For qRT-PCR, five switchgrass tissue samples were collected in triplicates. These tissues included seed, rachis, leaf, stem, and root. The *PveEF-1α*, *PvACT12*, and *PvUBQ6* were evaluated as internal reference genes (Gimeno et al., 2014). The *PvUBQ6* was selected because of its uniform expression levels in different tissues. The qRT-PCR results showed that the expression levels of PvTDIFL1 were in the rachis, which is consistent with the *in silico* data (Figure 3B). The expression of PvTDIFL3^{MR3} was relatively high in the rachis and leaf. In contrast, the expression of PvTDIFL3^{MR2} was more specific to the rachis (Figures 3C,D). However, the expression of PvTDIFL2 and PvTDIFL4 was undetectable, probably due to low levels of expression. The relatively high levels of expression in the rachis provides evidence for PvTDIFL genes contributing to vascular development, similar to the *Arabidopsis* TDIF genes.

In vitro PvTDIFL Peptide Treatment Increased Hypocotyl Stele Cell Numbers in *Arabidopsis*

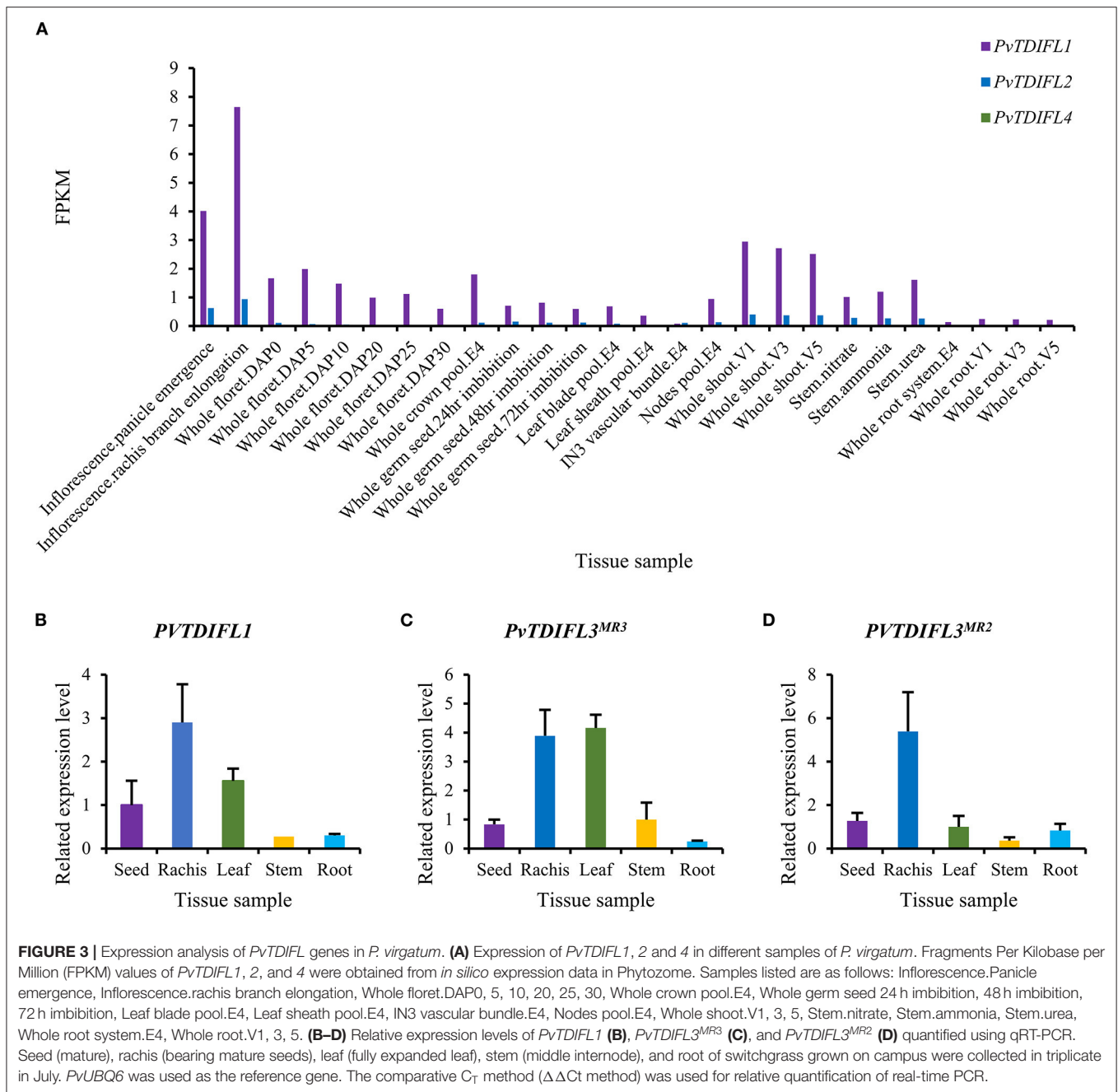
Exogenous TDIF peptide promotes procambial cell divisions, which leads to a remarkable increase in the vascular development of the hypocotyl in *Arabidopsis* (Hirakawa et al., 2010a). To study the activity and functional conservation of PvTDIFL peptides, four types of PvTDIFL peptides corresponding to the TDIFL

motifs from PvTDIFL1, PvTDIFL3^{MR3} and PvTDIFL3^{MR2} were chemically synthesized and exogenously applied to *Arabidopsis* seedlings, at a concentration of 10 μM. The *Arabidopsis* TDIF peptide was used as the positive control (Whitford et al., 2008).

Arabidopsis seedlings were grown in liquid MS media either with or without TDIF/TDIFL peptides for 10 d. To test whether these peptide treatments affected the vasculature of the hypocotyl, semi-thin transverse sections were prepared. The results showed that the application of *Arabidopsis* TDIF peptides induced increases in the size of the stele with significant increases in cell numbers, as previously reported (Figures 4A,B,G) (Whitford et al., 2008). Similarly, the number of cells in the stele increased significantly in the seedlings treated with PvTDIFL_1p, 2p, and 3p, but not as much as in the TDIF-treated seedlings (Figures 4A–E,G). In contrast, the PvTDIFL_4p treatment caused an unexpected decrease in the number of cells in the stele, due to the His (H) substitution for Asn (N) at the 12th residue of PvTDIFL_4p (Figures 4A,F,G). These data indicate that the activities of the three peptides (PvTDIFL_2p, 3p, and 4p) encoded by PvTDIFL3 diverged.

Influence of Heterologous Expression of PvTDIFL Genes on Plant Morphology and Vascular Development in *Arabidopsis*

As described above, PvTDIFL1, 3^{MR3} and 3^{MR2} differ in their motif numbers, motif sequences and peptide activities. To further investigate their functions in plant development, the 35S promoter was used to drive the expression of PvTDIFL1, 3^{MR3} and 3^{MR2} in *Arabidopsis*. The relative expression levels of the PvTDIFL transgenes in *Arabidopsis* were analyzed by RT-PCR (Figure 5A). The transgene expression levels and morphologies of two representative lines for each transgene were compared to Col-0. Four-week-old soil-grown plants were photographed (Figures 5B–H). In comparison with the wild-type plants (Figure 5B). Both lines harboring the 35S:PvTDIFL1 transgene developed smaller rosettes with small, round, and bushy leaves relative to Col-0 (Figures 5B–D). Similar results were obtained when *AtCLE42* and *44* were overexpressed in *Arabidopsis* (Strabala et al., 2006). In contrast, the morphological changes of 35S:PvTDIFL3^{MR3} and 35S:PvTDIFL3^{MR2} plants were less severe and less consistent (Figures 5E–H).



To further quantify the phenotypic changes of the 35S:*PvTDIFL* plants, the above-mentioned lines were grown on vertical plates for 2 weeks to observe the morphological changes in roots. A significant decrease in the length of the primary root was observed in all heterologous expression lines, except for line 35S:*PvTDIFL3^{MR2}*-1 (Figures 6A–G,O). Similar short-root phenotypes were observed in rice and pine after treatments with synthetic TDIF peptides (Kinoshita et al., 2007; Strabala et al., 2014). The heights of the inflorescence of 35S:*PvTDIFL* plants were measured after 6 weeks of growth in soil, 2 weeks after the initiation of flowering. Extreme dwarfism was observed in

the lines harboring the 35S:*PvTDIFL1* transgene. The heights of their inflorescences were 40% of the wild-type plants ($p \leq 0.001$, $n = 10$). The height of the inflorescence was also decreased in the lines harboring the 35S:*PvTDIFL3^{MR3}* transgene. The heights of the inflorescence from the line 35S:*PvTDIFL3^{MR3}*-1 and -2 were 54% ($p \leq 0.001$, $n = 10$) and 34% ($p \leq 0.001$, $n = 10$) of the wild type plants, respectively. In contrast, no significant decrease in the height of the inflorescence was observed in the lines harboring the 35S:*PvTDIFL3^{MR2}* transgene (Figures 6H–N,P).

To investigate the functions of *PvTDIFL* genes in vascular development, the hypocotyls of 6-week-old *Arabidopsis* were

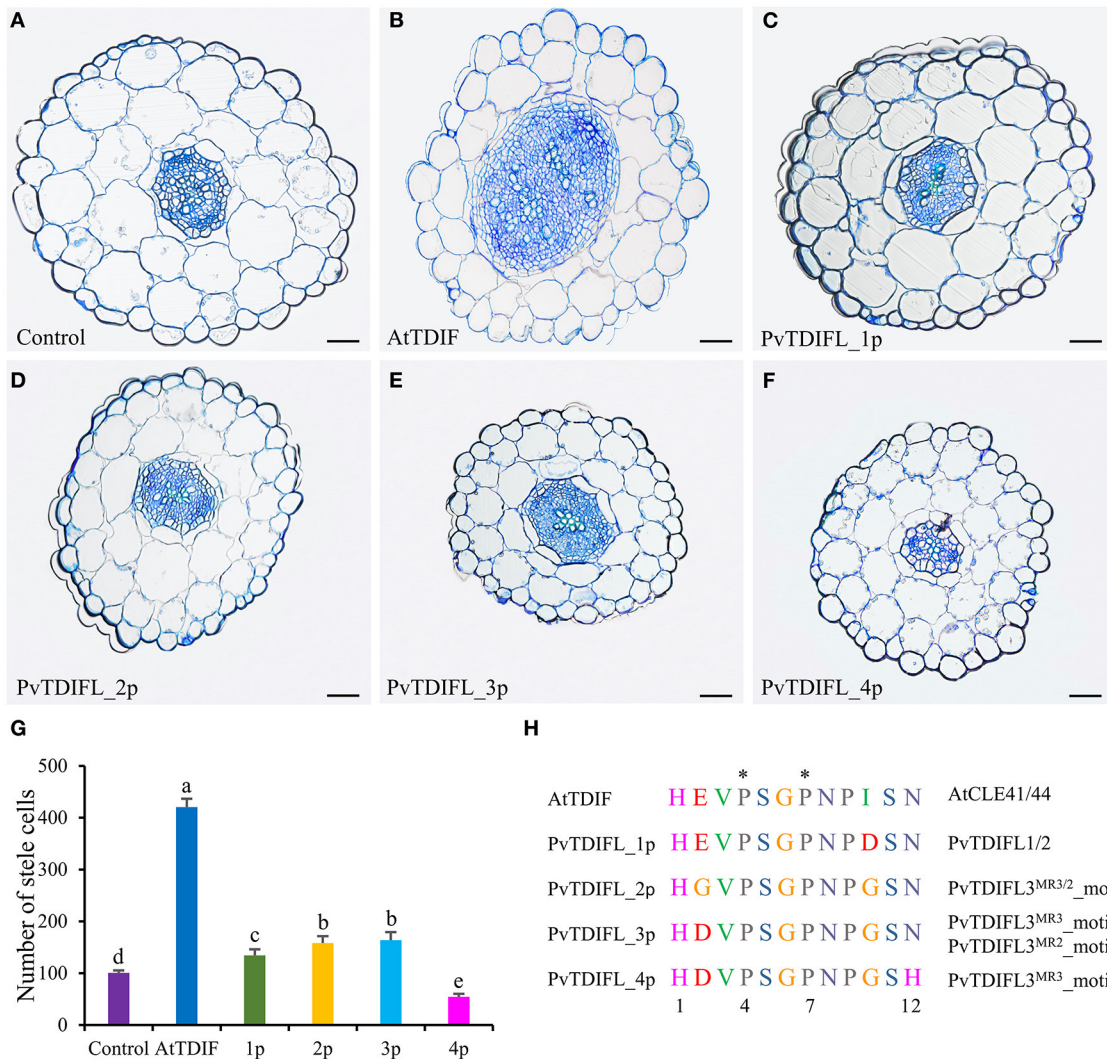


FIGURE 4 | Effects of AtTDIF and PvTDIFL peptides on stele development of 10-day-old *Arabidopsis* hypocotyls grown in liquid media. **(A)** Transverse section of hypocotyl from *Arabidopsis* plants without peptide-treatment. **(B–F)** Transverse sections of hypocotyls from *Arabidopsis* plants treated with the AtTDIF **(B)**, PvTDIFL_1p **(C)**, PvTDIFL_2p **(D)**, PvTDIFL_3p **(E)**, and PvTDIFL_4p **(F)** synthetic peptides. Sections were 2.5 μm thick and stained with 0.05% (w/v) aqueous toluidine blue. Bar = 50 μm . **(G)** Numbers of stele cells in the hypocotyls of non-treated and synthetic peptide-treated plants. Biological replicates were sections from 6 different hypocotyls. Different letters indicate statistically significant differences ($p < 0.05$), $n = 6$. **(H)** Sequences and modifications of AtTDIF and PvTDIFL peptides. Peptide names are indicated at the left. Proteins containing the indicated peptides are indicated at the right. The asterisk indicates hydroxyproline.

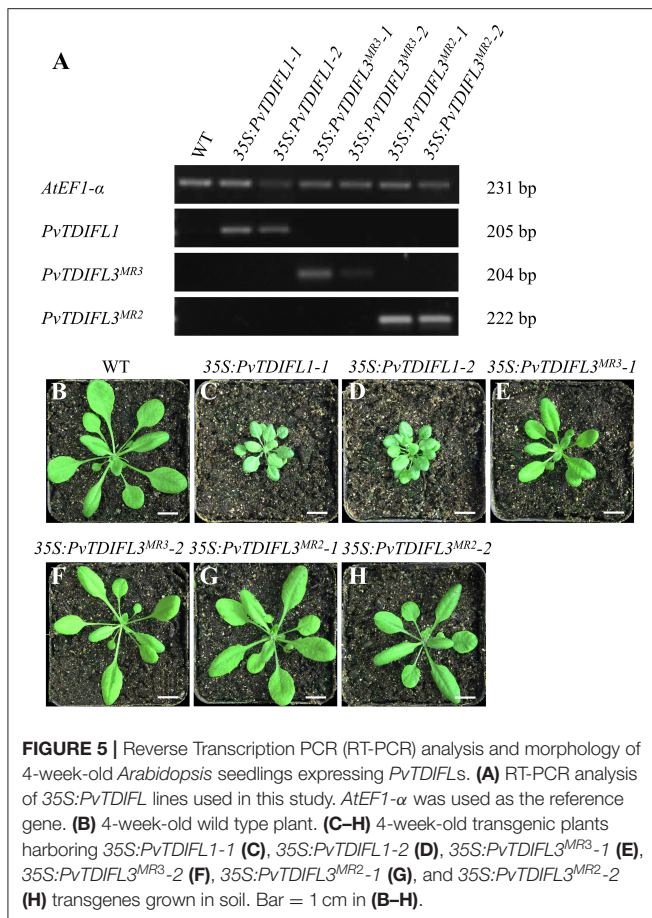
sectioned and analyzed using light microscopy. In comparison with Col-0 (**Figures 7A,E**), heterologous expression of *PvTDIFL1* induced a drastic increase in the number of cells in the stele, suppressed the differentiation of xylem and disrupted the organization of the vascular tissue (**Figures 7B,F**). Heterologous expression of *PvTDIFL3^{MR3}* induced a reduction in the size of xylem and an increase in the size of phloem without disrupting the organization of the vascular tissue and did not influence the diameter of the hypocotyl (**Figures 7C,G**). Heterologous expression of *PvTDIFL3^{MR2}* led to a similar albeit somewhat attenuated phenotype relative to the heterologous expression of *PvTDIFL1*. For instance, the size of tracheary elements was not reduced in the plants expressing *PvTDIFL3^{MR2}* (**Figures 7D,H**). The above results are consistent with the previous reports on

the *TDIF* genes in *Arabidopsis* and *Populus* (Hirakawa et al., 2008; Whitford et al., 2008; Etchells and Turner, 2010; Etchells et al., 2015; Li et al., 2018). Although *PvTDIFL1* contains only one single TDIFL motif, it had the greatest influence on vascular development. On the contrary, multiple TDIFL motifs did not increase the activity of either *PvTDIFL3^{MR3}* or *PvTDIFL3^{MR2}* relative to *PvTDIFL1*.

DISCUSSION

Identification of *TDIF/TDIFL* Genes in *P. virgatum*

In this study, 93 putative *CLE* genes were identified in the genome of *P. virgatum*, by using a novel method that was



recently developed (Zhang et al., 2020) followed by gene cloning. In *Arabidopsis*, all of the 32 *CLE* genes encode proteins with a single *CLE* motif, except for *CLE18*, which contains a second *CLEL* motif (Meng et al., 2012). Surprisingly, five *CLE* proteins containing multiple *CLE* motifs were identified in *O. sativa*, *T. aestivum*, and *Medicago truncatula* (Oelkers et al., 2008). A total of 59 *CLE* proteins in 27 plant species contain multiple *CLE* motifs (Goad et al., 2017). Genes encoding proteins containing multiple *CLE* motifs have been recently identified in various plants, despite that the *CLE* motifs from the same protein might or might not be identical to each other (Goad et al., 2017). Most functional studies on *CLE* genes have been conducted with genes encoding a single *CLE* motif. The knowledge of the *CLE* genes encoding multiple motifs remains limited. In this study of *CLE* genes in *P. virgatum*, it was found that three *PvCLE* genes—*Pavir.Fa00904.1*, *PvTDIFL3^{MR3}*, and *PvTDIFL3^{MR2}* encode proteins containing multiple *CLE* motifs, which allowed the functions of the *CLE* motif-containing proteins encoded by these genes to be studied.

Among the three *PvCLE*s that encode multiple *CLE* motifs, *PvTDIFL3^{MR3}* and *3^{MR2}* appear to encode *CLE* peptides that are homologous to the *TDIF* peptide. The function of the *TDIF* peptide in vascular development has been well-studied in several species, such as *Arabidopsis*, *Populus*, *Marchantia polymorpha*

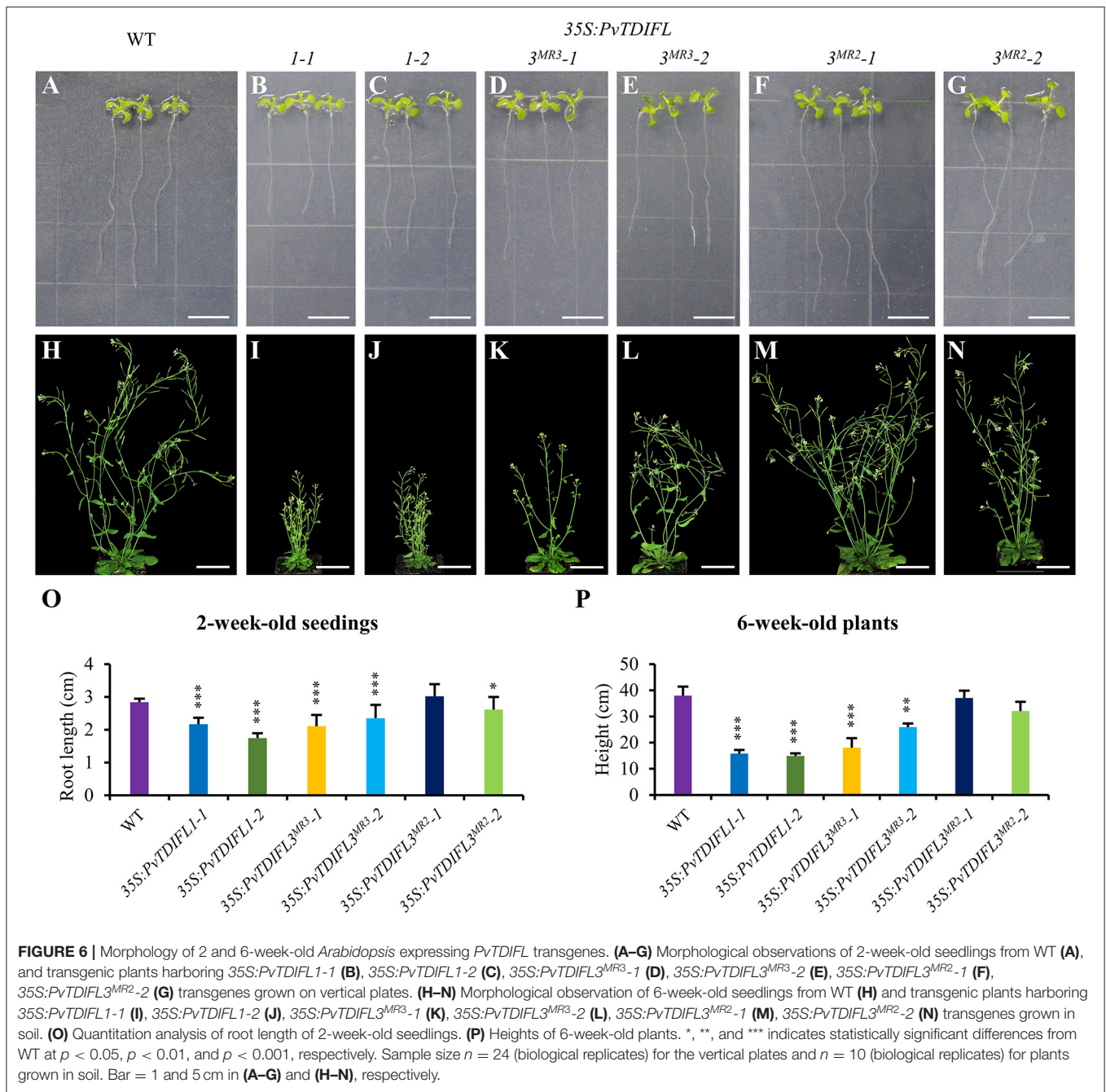
(Ito et al., 2006; Hirakawa et al., 2008, 2010a,b; Etchells and Turner, 2010; Etchells et al., 2015; Kondo and Fukuda, 2015). However, these previously studied *TDIF/TDIFL* genes encode a single *TDIF/TDIFL* motif. Therefore, functional analysis of the *TDIFL* peptides from the *PvTDIFL3^{MR3}* and *3^{MR2}* proteins could provide a better understanding of the regulatory activities of *TDIF/TDIFL* peptides.

In total, five *PvTDIFL*-encoding genes were identified in *P. virgatum*. The motif sequences of *PvTDIFL1/2* and *TDIF* are very similar. Indeed, only the 10th amino acid residue of the motif is different between *PvTDIFL1/2* and *TDIF*. The *TDIFL* peptide from *PvTDIFL1/2* represents the largest group of *TDIF/TDIFL* peptides in monocots (Zhang et al., 2020). The number of different residues in the *TDIFL* motifs of *PvTDIFL3^{MR3}*, *3^{MR2}*, and 4 ranges from two to three (Figures 2B,C). The *PvTDIFL3^{MR3}* and *3^{MR2}* contain three and two *TDIFL* motifs, respectively. Sequence alignments of *PvTDIFL* proteins show that *PvTDIFL3^{MR3}* had one more repeat of the *TDIFL* motif within its flanking sequence relative to *PvTDIFL3^{MR2}*. The *PvTDIFL3^{MR2}* was a “byproduct” of cloning *PvTDIFL3^{MR3}* by using gene specific primers for *PvTDIFL3^{MR3}*. Meanwhile, *PvTDIFL3^{MR3}* and *3^{MR2}* were matched to the same chromosomal locus, which provides evidence that these two genes could be alleles. An alternative explanation is that *PvTDIFL3^{MR2}* is simply missing from the v1.1 genome sequence of *P. virgatum*.

Activities of *PvTDIFL* Peptides in *Arabidopsis*

Alanine scanning mutagenesis indicated that the 2nd, 5th, 7th, 10th, and 11th residues of the *TDIF* motif do not contribute to its activity. However, the H¹, V³, G⁶, N⁸, P⁹, and N¹² substitutions caused severe losses of *TDIF* activity (Ito et al., 2006). In order to investigate the activities of *PvTDIFL* peptides based on the predicted motifs, four *PvTDIFL* peptides were synthesized and applied to *Arabidopsis* seedlings. The peptide activities were evaluated based on their ability to influence cell numbers and cell arrangement in the vasculature of the hypocotyl.

The results showed that *PvTDIFL_1p*, *2p*, and *3p* had similar and significant activities in promoting cell division, disrupting vascular cell patterns and inhibiting xylem development, although their activities were weaker than the *Arabidopsis* *TDIF* peptide (Figures 4A–E,G). On the contrary, *PvTDIFL_4p* (corresponding to the 2nd motif of *PvTDIFL3^{MR3}*) had no *TDIF* activity. Instead, *PvTDIFL_4p* induced a 50% reduction in the number of cells in the hypocotyl, which is consistent with *PvTDIFL_4p* serving as an antagonist of peptides that possess *TDIF* activity (Figures 4E,G). The sequence alignment of the *PvTDIFL* peptides that included the *TDIF* peptide showed that *PvTDIFL_1p*, *2p*, and *3p* have different residues at the 2nd and/or 10th residues, which are not critical positions for *TDIF* activity (Ito et al., 2006). The *PvTDIFL_4p* has an extra substitution, with a His (H) instead of an Asn (N) at the 12th residue (Figure 4H), which is one of the critical positions (Ito et al., 2006). This H-to-N substitution is consistent with its inhibitory activity in the exogenous peptide treatment experiments.



Functional Analysis of *PvTDIFL* Genes in *Arabidopsis*

It has been hypothesized that a full CLE protein precursor carrying multiple motifs can release several active peptides after processing, which could play an amplification effect (Oelkers et al., 2008). To better understand the function of *PvTDIFL* genes, *PvTDIFL*1 (one motif), *PvTDIFL*3^{MR3} (three motifs), and *PvTDIFL*3^{MR2} (two motifs) were expressed in *Arabidopsis*. Heterologous expression of *PvTDIFL*1 mimicked the phenotypes of the *Arabidopsis* plants that overexpressed the endogenous *TDIF* genes, such as *CLE41* and *CLE44* (Strabala et al., 2006;

Etchells and Turner, 2010). However, heterologous expression of *PvTDIFL*3^{MR3} and 3^{MR2} produced more subtle phenotypes than the heterologous expression of *PvTDIFL*1 (Figures 5–7). An amplification of TDIFL activity in *Arabidopsis* plants expressing *PvTDIFL*3^{MR3} or 3^{MR2} was not observed although these genes encode peptides with multiple motifs. The lack of the amplification effect has several possible explanations. Firstly, *PvTDIFL*3^{MR3} and 3^{MR2} were heterologously expressed in *Arabidopsis*. Because *Arabidopsis* does not have any CLE proteins with multiple CLE motifs, it might not be able to process *PvTDIFL*3^{MR3} or 3^{MR2} protein precursors efficiently. Secondly,

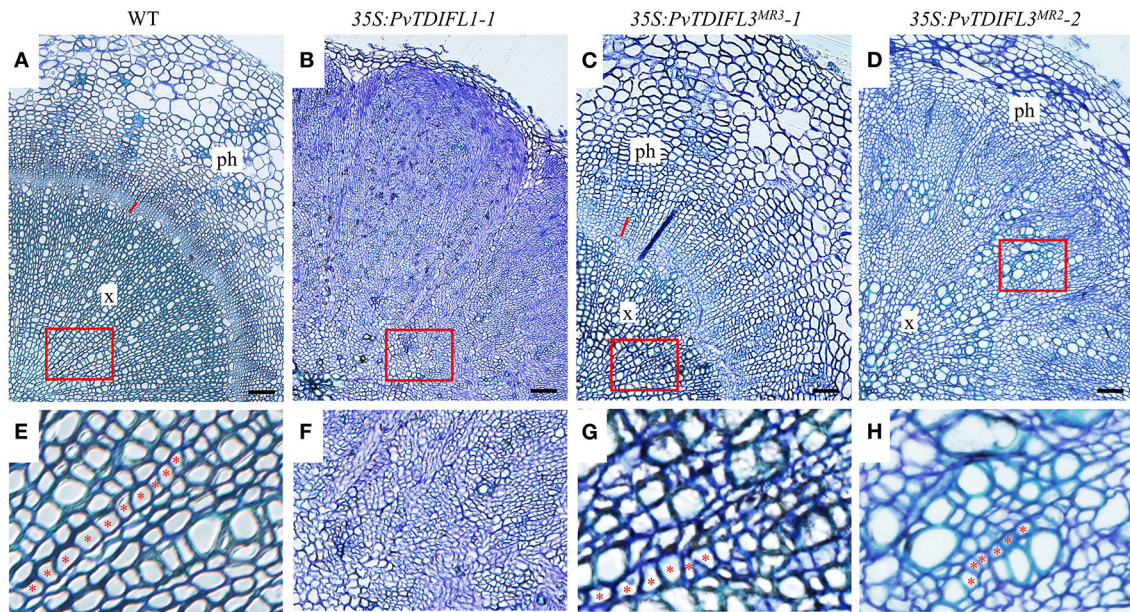


FIGURE 7 | Histology of 6-week-old *Arabidopsis* lines expressing *PvTDIFL* transgenes. **(A–D)** Histological observation of hypocotyls from WT **(A)** and transgenic seedlings harboring 35S:*PvTDIFL1-1* **(B)**, 35S:*PvTDIFL3^{MR3-1}* **(C)**, and 35S:*PvTDIFL3^{MR2-2}* **(D)** transgenes. Transverse sections that were 2.5 μm thick were stained with 0.05% (w/v) aqueous toluidine blue. Bar = 50 μm . x and ph indicate xylem and phloem, respectively. The red line indicates cambium in **(A)** and **(C)**. **(E–H)** High magnification images from the areas in red boxes from **(A–D)**, respectively. Red asterisks show examples of organized files of cells.

the motif sequences of PvTDIFL peptides are not the same as the endogenous TDIF/TDIFL peptides of *Arabidopsis*. Therefore, the affinity of the PXY/TDR receptor in *Arabidopsis* for the PvTDIFL peptides is difficult to predict and requires more experimentation to understand. Thirdly, although the typical sequence of the TDIF peptide is HEVPSGPNPISN (Ito et al., 2006), the conserved sequences flanking the TDIFL motifs from PvTDIFL3^{MR3} and 3^{MR2} provide evidence that possible variants of the mature motifs are encoded by these two genes. Finally, the experiments in this study have multiple variables, therefore it is hard to know whether all the TDIFL motifs from PvTDIFL3^{MR3} and 3^{MR2} have been successfully processed. The proteomics analysis of small proteins based on liquid chromatography with tandem mass spectrometry (LC-MS/MS) technique (Wang et al., 2020) can be applied to the analysis of transgenic lines harboring the transgenes that encode multiple PvTDIFL motifs with various alanine substitutions. This may help to analyze the processing of multiple PvTDIFL motifs.

The PvTDIFL3^{MR3} contains a 47-amino acids insertion between the amino acid residues 77 and 123. This insertion introduces an extra TDIFL motif in PvTDIFL3^{MR3} relative to PvTDIFL3^{MR2} (Figure 2C). The extra TDIFL motif is corresponding to PvTDIFL_4p (Figure 4H). A moderate TDIF-overexpression phenotype was apparent in the hypocotyl sections of the 6-week-old 35S:*PvTDIFL3^{MR2}* plants, which provides evidence that at least one of the PvTDIFL peptides (motif 1 and motif 3) was successfully processed. On the contrary, although vascular development in 35S:*PvTDIFL3^{MR3}* plants was reduced, the vascular organization of the hypocotyl was well maintained. These data suggest a processing of motif

2 from PvTDIFL3^{MR3} and indicate that PvTDIFL_4P may serve as an antagonist of PvTDIFL_2P (PvTDIFL3^{MR3}_motif 1), PvTDIFL_3P (PvTDIFL3^{MR3}_motif 3), and the endogenous TDIF peptide. The inhibitory effect derived from motif 2 of PvTDIFL3^{MR3} in the *PvTDIFL3^{MR3}* heterologous expression experiments is consistent with the inhibition of stele development by PvTDIFL_4p that was observed during the exogenous peptide treatments in 10-day-old *Arabidopsis* seedlings (Figures 4F,G).

Previous reports showed that although TDIF has no inhibitory effect on root elongation in *Arabidopsis* (Ito et al., 2006; Whitford et al., 2008), TDIF mildly inhibits root elongation in rice and pine (Kinoshita et al., 2007; Strabala et al., 2014). In this study, heterologous expression of *PvTDIFLs* significantly shortened the roots of *Arabidopsis*, especially in the 35S:*PvTDIFL1* lines (Figures 6A–G). These data are consistent with the diversification of *TDIF/TDIFL* gene function in different species. However, little is known about the mechanism responsible for these differences in peptide activity.

Tissue-Specific Expression of *TDIF* to Increase Biomass in Plant

As a PBC, *P. virgatum* is a commonly used material to study the synthesis of biomass. In this study, heterologous expression of *PvTDIFLs* in *Arabidopsis* caused dwarf seedlings and a disordered vasculature, indicating that constitutive heterologous expression of *PvTDIFLs* reduced biomass. It is consistent with the previous studies on overexpression of the endogenous *TDIF* genes in *Arabidopsis* (Hirakawa et al., 2008; Whitford et al., 2008; Etchells

and Turner, 2010). However, the phloem-specific expression of *PttCLE41* leads to increased woody biomass in *Populus* and thus, demonstrates that it is possible to increase the biomass by manipulating the TDIF–PXY/TDR signaling module in plants (Etchells et al., 2015). In hybrid poplar, the *PttWOX4* genes act downstream of PXY/TDR to control cell division activity in the vascular cambium and hence, to increase stem girth (Kucukoglu et al., 2017). Overexpression of the *WOX* gene *STF* (*STENOFOLIA*) improves biomass yields in grasses (Wang et al., 2017). In this study, five TDIF/TDIFL genes in *P. virgatum* were identified. Three of these genes in *Arabidopsis* were cloned and heterologous expressed. Overexpression technologies and exogenous peptide treatment experiments gave a better understanding of the functions and activities of various TDIFL peptides, including PvTDIFL peptides, and also provide clues that will drive future applied research on biomass improvement by manipulating the TDIF–PXY/TDR–WOX4 signaling pathway in plants.

CONCLUSION

In this study, 93 genes that are homologous to *CLE* were identified in *P. virgatum* and were divided into 6 groups based on a phylogenetic analysis. A total of five PvCLE members were assigned to the fourth group that consisted of the H-type CLEs. The five genes that were most similar to *Arabidopsis* TDIF were named *PvTDIFL1*, *PvTDIFL2*, *PvTDIFL3^{MR3}*, *PvTDIFL3^{MR2}*, and *PvTDIFL4*. *PvTDIFL3^{MR3}* and *3^{MR2}* contain three and two TDIFL peptide motifs, respectively. Expression analysis showed that *PvTDIFL* genes were highly expressed in the rachis, which is rich in vascular tissue. Experiments with exogenous polypeptides demonstrated that, apart from PvTDIFL_4p, the ability to influence the development of the stele in the hypocotyl is conserved in both PvTDIFL and *Arabidopsis* TDIF peptides. The heterologous expression of *PvTDIFL1*, *3^{MR3}*, and *3^{MR2}* all affected the growth of *Arabidopsis* plants and the development of the vascular tissue in the hypocotyl to varying degrees. The *Arabidopsis* plants that stably expressed *PvTDIFL3^{MR3}* and *3^{MR2}* did not develop elevated levels of CLE peptide activity that might be expected from the multiple CLE motifs contained in the proteins encoded by these genes. At present, there are few studies on the processing and activity of plant CLEs containing multiple motifs. This study will shape future

work that aims to increase biomass by modifying the TDIF signaling pathway.

DATA AVAILABILITY STATEMENT

The datasets presented in this study can be found in online repositories. The names of the repository/repositories and accession number(s) can be found in the article/**Supplementary Material**.

AUTHOR CONTRIBUTIONS

BZ and XS conceived and designed the experiments. XS, ZZ, and LL identified the *PvCLE* genes. LL, KD, JT, and DT performed the experiments and analyzed the corresponding results. DT drafted the manuscript. RL, BZ, and XS revised this manuscript. All authors contributed to the article and approved the submitted version.

FUNDING

This work was supported by the Fundamental Research Funds for the Central Universities (2662020YLPY026, 2662018PY071), and the National Natural Science Foundation of China (31770639, 31370673).

SUPPLEMENTARY MATERIAL

The Supplementary Material for this article can be found online at: <https://www.frontiersin.org/articles/10.3389/fpls.2021.737219/full#supplementary-material>

Supplementary Figure 1 | Nucleotide sequences of *PvTDIFL3^{MR3}* and *PvTDIFL3^{MR2}*. The nucleotide sequences were obtained by clones. Green, blue, and pink font represent 5'-UTR, CDS, and 3'-UTR, respectively. The sequences corresponding to the TDIFL motifs are underlined.

Supplementary Figure 2 | Weblogo images of CLE motifs from six groups in *Arabidopsis* and switchgrass. Weblogo images were created by using the Weblogo online tool with the amino acid sequences from the predicted CLE motifs.

Supplementary Table 1 | Amino acid sequences from TDIF/TDIFL used for chemical synthesis.

Supplementary Table 2 | Primers used in this study.

Supplementary Table 3 | Information of PvCLE proteins identified in this study.

REFERENCES

- Bjellqvist, B., Hughes, G. J., Pasquali, C., Paquet, N., Ravier, F., Sanchez, J. C., et al. (1993). The focusing positions of polypeptides in immobilized pH gradients can be predicted from their amino-acid-sequences. *Electrophoresis* 14, 1023–1031. doi: 10.1002/elps.11501401163
- Chen, Q., and Song, G. Q. (2019). Protocol for agrobacterium-mediated transformation and transgenic plant production of switchgrass. *Methods Mol. Biol.* 1864, 105–115. doi: 10.1007/978-1-4939-8778-8_8
- Clifton-Brown, J., Harfouche, A., Casler, M. D., Jones, H. D., Macalpine, W. J., Murphy-Bokern, D., et al. (2019). Breeding progress and preparedness for mass-scale deployment of perennial lignocellulosic biomass crops switchgrass, miscanthus, willow and poplar. *GCB Bioenergy* 11, 118–151. doi: 10.1111/gcbb.12566
- Clough, S. J., and Bent, A. F. (1998). Floral dip: a simplified method for *Agrobacterium*-mediated transformation of *Arabidopsis thaliana*. *Plant J.* 16, 735–743. doi: 10.1046/j.1365-313x.1998.00343.x
- Cock, J. M., and McCormick, S. (2001). A large family of genes that share homology with *CLAVATA3*. *Plant Physiol.* 126, 939–942. doi: 10.1104/pp.126.3.939
- Crooks, G. E., Hon, G., Chandonia, J. M., and Brenner, S. E. (2004). WebLogo: a sequence logo generator. *Genome Res.* 14, 1188–1190. doi: 10.1101/gr.849004
- Etchells, J. P., Mishra, L. S., Kumar, M., Campbell, L., and Turner, S. R. (2015). Wood formation in trees is increased by manipulating PXY-regulated cell division. *Curr. Biol.* 25, 1050–1055. doi: 10.1016/j.cub.2015.02.023

- Etchells, J. P., Provost, C. M., Mishra, L., and Turner, S. R. (2013). *WOX4* and *WOX14* act downstream of the PXY receptor kinase to regulate plant vascular proliferation independently of any role in vascular organisation. *Development* 140, 2224–2234. doi: 10.1242/dev.091314
- Etchells, J. P., Smit, M. E., Gaudinier, A., Williams, C. J., and Brady, S. M. (2016). A brief history of the TDIF-PXY signalling module: balancing meristem identity and differentiation during vascular development. *New Phytol.* 209, 474–484. doi: 10.1111/nph.13642
- Etchells, J. P., and Turner, S. R. (2010). The PXY-CLE41 receptor ligand pair defines a multifunctional pathway that controls the rate and orientation of vascular cell division. *Development* 137, 767–774. doi: 10.1242/dev.044941
- Fiers, M., Golemic, E., Xu, J., van der Geest, L., Heidstra, R., Stiekema, W., et al. (2005). The 14-amino acid CLV3, CLE19, and CLE40 peptides trigger consumption of the root meristem in *Arabidopsis* through a CLAVATA2-dependent pathway. *Plant Cell* 17, 2542–2553. doi: 10.1105/tpc.105.034009
- Fiers, M., Ku, K. L., and Liu, C. M. (2007). CLE peptide ligands and their roles in establishing meristems. *Curr. Opin. Plant Biol.* 10, 39–43. doi: 10.1016/j.pbi.2006.11.003
- Fisher, K., and Turner, S. (2007). PXY, a receptor-like kinase essential for maintaining polarity during plant vascular-tissue development. *Curr. Biol.* 17, 1061–1066. doi: 10.1016/j.cub.2007.05.049
- Fletcher, L. C., Brand, U., Running, M. P., Simon, R., and Meyerowitz, E. M. (1999). Signaling of cell fate decisions by CLAVATA3 in *Arabidopsis* shoot meristems. *Science* 283, 1911–1914. doi: 10.1126/science.283.5409.1911
- Gimeno, J., Eattock, N., Van Deynze, A., and Blumwald, E. (2014). Selection and validation of reference genes for gene expression analysis in switchgrass (*Panicum virgatum*) using quantitative real-time RT-PCR. *PLoS ONE* 9:e91474. doi: 10.1371/journal.pone.0091474
- Goad, D. M., Zhu, C., and Kellogg, E. A. (2017). Comprehensive identification and clustering of *CLV3/ESR-related* (CLE) genes in plants finds groups with potentially shared function. *New Phytol.* 216, 605–616. doi: 10.1111/nph.14348
- Goodstein, D. M., Shu, S., Howson, R., Neupane, R., Hayes, R. D., Fazo, J., et al. (2012). Phytome: a comparative platform for green plant genomics. *Nucleic Acids Res.* 40, D1178–1186. doi: 10.1093/nar/gkr944
- Hall, B. G. (2013). Building phylogenetic trees from molecular data with MEGA. *Mol. Biol. Evol.* 30, 1229–1235. doi: 10.1093/molbev/mst012
- Han, H., Zhang, G., Wu, M., and Wang, G. (2016). Identification and characterization of the *Populus trichocarpa* CLE family. *BMC Genomics* 17:174. doi: 10.1186/s12864-016-2504-x
- Hirakawa, Y., Kondo, Y., and Fukuda, H. (2010a). Regulation of vascular development by CLE peptide-receptor systems. *J. Integr. Plant Biol.* 52, 8–16. doi: 10.1111/j.1744-7909.2010.00904.x
- Hirakawa, Y., Kondo, Y., and Fukuda, H. (2010b). TDIF peptide signaling regulates vascular stem cell proliferation via the *WOX4* homeobox gene in *Arabidopsis*. *Plant Cell* 22, 2618–2629. doi: 10.1105/tpc.110.076083
- Hirakawa, Y., Shinohara, H., Kondo, Y., Inoue, A., Nakanomyo, I., Ogawa, M., et al. (2008). Non-cell-autonomous control of vascular stem cell fate by a CLE peptide/receptor system. *Proc. Natl. Acad. Sci. U.S.A.* 105, 15208–15213. doi: 10.1073/pnas.0808444105
- Hu, B., Jin, J., Guo, A. Y., Zhang, H., Luo, J., and Gao, G. (2015). GSDS 2.0: an upgraded gene feature visualization server. *Bioinformatics* 31, 1296–1297. doi: 10.1093/bioinformatics/btu817
- Ito, Y., Nakanomyo, I., Motose, H., Iwamoto, K., Sawa, S., Dohmae, N., et al. (2006). Dodeca-CLE peptides as suppressors of plant stem cell differentiation. *Science* 313, 842–845. doi: 10.1126/science.1128436
- Karimi, M., Inze, D., and Depicker, A. (2002). GATEWAY(TM) vectors for *Agrobacterium*-mediated plant transformation. *Trends Plant Sci.* 7, 193–195. doi: 10.1016/S1360-1385(02)02251-3
- Keshwani, D. R., and Cheng, J. J. (2009). Switchgrass for bioethanol and other value-added applications: a review. *Bioresour. Technol.* 100, 1515–1523. doi: 10.1016/j.biortech.2008.09.035
- Kinoshita, A., Nakamura, Y., Sasaki, E., Kyoizuka, J., Fukuda, H., and Sawa, S. (2007). Gain-of-function phenotypes of chemically synthetic CLAVATA3/ESR-related (CLE) peptides in *Arabidopsis thaliana* and *Oryza sativa*. *Plant Cell Physiol.* 48, 1821–1825. doi: 10.1093/pcp/pcm154
- Kondo, T., Sawa, S., Kinoshita, A., Mizuno, S., Kakimoto, T., Fukuda, H., et al. (2006). A plant peptide encoded by *CLV3* identified by *in situ* MALDI-TOF MS analysis. *Science* 313, 845–848. doi: 10.1126/science.1128439
- Kondo, Y., and Fukuda, H. (2015). The TDIF signaling network. *Curr. Opin. Plant Biol.* 28, 106–110. doi: 10.1016/j.pbi.2015.10.002
- Kucukoglu, M. (2020). A novel NAC domain transcription factor *XVP* controls the balance of xylem formation and cambial cell divisions. *New Phytol.* 226, 5–7. doi: 10.1111/nph.16400
- Kucukoglu, M., Nilsson, J., Zheng, B., Chaabouni, S., and Nilsson, O. (2017). *WUSCHEL-RELATED HOMEBOX4* (*WOX4*)-like genes regulate cambial cell division activity and secondary growth in *Populus* trees. *New Phytol.* 215, 642–657. doi: 10.1111/nph.14631
- Letunic, I., and Bork, P. (2018). 20 years of the SMART protein domain annotation resource. *Nucleic Acids Res.* 46, D493–D496. doi: 10.1093/nar/gkx922
- Li, X., Yang, H., Wang, C., Yang, S., and Wang, J. (2018). Distinct transgenic effects of poplar *TDIF* genes on vascular development in *Arabidopsis*. *Plant Cell Rep.* 37, 799–808. doi: 10.1007/s00299-018-2268-7
- Li, Z., Liu, G., Zhang, J., Zhang, J., and Bao, M. (2008). Extraction of high-quality tissue-specific RNA from London plane trees (*Platanus acerifolia*), permitting the construction of a female inflorescence cDNA library. *Funct. Plant Biol.* 35, 159–165. doi: 10.1071/FP07212
- McLaughlin, S. B., and Adams Kszos, L. (2005). Development of switchgrass (*Panicum virgatum*) as a bioenergy feedstock in the United States. *Biomass Bioenergy* 28, 515–535. doi: 10.1016/j.biombioe.2004.05.006
- Meng, L., Buchanan, B. B., Feldman, L. J., and Luan, S. (2012). CLE-like (CLEL) peptides control the pattern of root growth and lateral root development in *Arabidopsis*. *Proc. Natl. Acad. Sci. U.S.A.* 109, 1760–1765. doi: 10.1073/pnas.1119864109
- Oelkers, K., Goffard, N., Weiller, G. F., Gresshoff, P. M., Mathesius, U., and Frickey, T. (2008). Bioinformatic analysis of the CLE signaling peptide family. *BMC Plant Biol.* 8:1. doi: 10.1186/1471-2229-8-1
- Ogawa-Ohnishi, M., Matsushita, W., and Matsubayashi, Y. (2013). Identification of three hydroxyproline O-arabinosyltransferases in *Arabidopsis thaliana*. *Nat. Chem. Biol.* 9, 726–730. doi: 10.1038/nchembio.1351
- Ohyama, K., Ogawa, M., and Matsubayashi, Y. (2008). Identification of a biologically active, secreted peptide in *Arabidopsis* by *in silico* gene screening, followed by LC-MS-based structure analysis. *Plant J.* 55, 152–160. doi: 10.1111/j.1365-313X.2008.03464.x
- Ohyama, K., Shinohara, H., Ogawa-Ohnishi, M., and Matsubayashi, Y. (2009). A glycopeptide regulating stem cell fate in *Arabidopsis thaliana*. *Nat. Chem. Biol.* 5, 578–580. doi: 10.1038/nchembio.182
- Ondzighi-Assoume, C. A., Willis, J. D., Ouma, W. K., Allen, S. M., King, Z., Parrott, W. A., et al. (2019). Embryogenic cell suspensions for high-capacity genetic transformation and regeneration of switchgrass (*Panicum virgatum* L.). *Biotechnol. Biofuels* 12:290. doi: 10.1186/s13068-019-1632-3
- Parrish, D. J., and Fike, J. H. (2005). The biology and agronomy of switchgrass for biofuels. *Crit. Rev. Plant Sci.* 24, 423–459. doi: 10.1080/07352680500316433
- Pfaffl, M. W. (2001). A new mathematical model for relative quantification in real-time RT-PCR. *Nucleic Acids Res.* 29:e45. doi: 10.1093/nar/29.9.e45
- Ragni, L., and Hardtke, C. S. (2014). Small but thick enough—the *Arabidopsis* hypocotyl as a model to study secondary growth. *Physiol. Plantarum* 151, 164–171. doi: 10.1111/ppl.12118
- Sanderson, M. A., Adler, P. R., Boateng, A. A., Casler, M. D., and Sarath, G. (2006). Switchgrass as a biofuels feedstock in the USA. *Can. J. Plant Sci.* 86, 1315–1325. doi: 10.4141/P06-136
- Sanderson, M. A., Reed, R. L., McLaughlin, S. B., Wullschlegel, S. D., Conger, B. V., Parrish, D. J., et al. (1996). Switchgrass as a sustainable bioenergy crop. *Bioresour. Technol.* 56, 83–93. doi: 10.1016/0960-8524(95)00176-X
- Sawa, S., Kinoshita, A., Betsuyaku, S., and Fukuda, H. (2008). A large family of genes that share homology with CLE domain in *Arabidopsis* and rice. *Plant Signal. Behav.* 3, 337–339. doi: 10.4161/psb.3.5.5344
- Schoof, H., Lenhard, M., Haecker, A., Mayer, K. F. X., Jurgens, G., and Laux, T. (2000). The stem cell population of *Arabidopsis* shoot meristems is maintained by a regulatory loop between the *CLAVATA* and *WUSCHEL* genes. *Cell* 100, 635–644. doi: 10.1016/S0092-8674(00)80700-X
- Solovyev, V., Kosarev, P., Seledsov, I., and Vorobyev, D. (2006). Automatic annotation of eukaryotic genes, pseudogenes and promoters. *Genome Biol.* 7(Suppl. 1):S10.1–12. doi: 10.1186/gb-2006-7-s1-s10
- Stahl, Y., Wink, R. H., Ingram, G. C., and Simon, R. (2009). A signaling module controlling the stem cell niche in *Arabidopsis* root meristems. *Curr. Biol.* 19, 909–914. doi: 10.1016/j.cub.2009.03.060

- Strabala, T. J., O'Donnell, P., J., Smit, A. M., Ampomah-Dwamena, C., Martin, E. J., et al. (2006). Gain-of-function phenotypes of many *CLAVATA3/ESR* genes, including four new family members, correlate with tandem variations in the conserved *CLAVATA3/ESR* domain. *Plant Physiol.* 140, 1331–1344. doi: 10.1104/pp.105.075515
- Strabala, T. J., Phillips, L., West, M., and Stanbra, L. (2014). Bioinformatic and phylogenetic analysis of the *CLAVATA3/EMBRYO-SURROUNDING REGION (CLE)* and the *CLE-LIKE* signal peptide genes in the *Pinophyta*. *BMC Plant Biol.* 14:47. doi: 10.1186/1471-2229-14-47
- Ursache, R., Nieminen, K., and Helariutta, Y. (2013). Genetic and hormonal regulation of cambial development. *Physiol. Plantarum* 147, 36–45. doi: 10.1111/j.1399-3054.2012.01627.x
- Wang, H., Niu, L., Fu, C., Meng, Y., Sang, D., Yin, P., et al. (2017). Overexpression of the *WOX* gene *STENOFOLIA* improves biomass yield and sugar release in transgenic grasses and display altered cytokinin homeostasis. *PLoS Genet.* 13:e1006649. doi: 10.1371/journal.pgen.1006649
- Wang, J., Kucukoglu, M., Zhang, L., Chen, P., Decker, D., Nilsson, O., et al. (2013). The *Arabidopsis* LRR-RLK, PXC1, is a regulator of secondary wall formation correlated with the TDIF-PXY/TDR-WOX4 signaling pathway. *BMC Plant Biol.* 13:94. doi: 10.1186/1471-2229-13-94
- Wang, P., Wang, Y., and Ren, F. (2019). Genome-wide identification of the *CLAVATA3/EMBRYO SURROUNDING REGION (CLE)* family in grape (*Vitis vinifera* L.). *BMC Genomics* 20:553. doi: 10.1186/s12864-019-5944-2
- Wang, S., Tian, L., Liu, H., Li, X., Zhang, J., Chen, X., et al. (2020). Large-scale discovery of non-conventional peptides in Maize and Arabidopsis through an integrated peptidogenomic pipeline. *Mol. Plant* 13, 1078–1093. doi: 10.1016/j.molp.2020.05.012
- Whitford, R., Fernandez, A., De Groot, R., Ortega, E., and Hilson, P. (2008). Plant CLE peptides from two distinct functional classes synergistically induce division of vascular cells. *Proc. Natl. Acad. Sci. U.S.A.* 105, 18625–18630. doi: 10.1073/pnas.0809395105
- Xi, Y., Ge, Y., and Wang, Z. Y. (2009). Genetic transformation of switchgrass. *Methods Mol. Biol.* 581, 53–59. doi: 10.1007/978-1-60761-214-8_4
- Yang, J. H., Lee, K.-H., Du, Q., Yang, S., Yuan, B., Qi, L., et al. (2020). A membrane-associated NAC domain transcription factor *XVP* interacts with TDIF co-receptor and regulates vascular meristem activity. *New Phytol.* 226, 59–74. doi: 10.1111/nph.16289
- Zhang, H., Lin, X., Han, Z., Wang, J., Qu, L. J., and Chai, J. (2016). SERK family receptor-like kinases function as co-receptors with PXY for plant vascular development. *Mol. Plant* 9, 1406–1414. doi: 10.1016/j.molp.2016.07.004
- Zhang, J., Elo, A., and Helariutta, Y. (2011). Arabidopsis as a model for wood formation. *Curr. Opin. Biotechnol.* 22, 293–299. doi: 10.1016/j.copbio.2010.11.008
- Zhang, Z., Liu, L., Kucukoglu, M., Tian, D., Larkin, R. M., Shi, X., et al. (2020). Predicting and clustering plant *CLE* genes with a new method developed specifically for short amino acid sequences. *BMC Genomics* 21:709. doi: 10.1186/s12864-020-07231-4

Conflict of Interest: The authors declare that the research was conducted in the absence of any commercial or financial relationships that could be construed as a potential conflict of interest.

Publisher's Note: All claims expressed in this article are solely those of the authors and do not necessarily represent those of their affiliated organizations, or those of the publisher, the editors and the reviewers. Any product that may be evaluated in this article, or claim that may be made by its manufacturer, is not guaranteed or endorsed by the publisher.

Copyright © 2021 Tian, Tang, Luo, Zhang, Du, Larkin, Shi and Zheng. This is an open-access article distributed under the terms of the Creative Commons Attribution License (CC BY). The use, distribution or reproduction in other forums is permitted, provided the original author(s) and the copyright owner(s) are credited and that the original publication in this journal is cited, in accordance with accepted academic practice. No use, distribution or reproduction is permitted which does not comply with these terms.